Eur. Phys. J. B **39**, 77–85 (2004)
DOI: 10.1140/epjb/e2004-00173-2

THE EUROPEAN PHYSICAL JOURNAL B

Torsional stiffness of viscoelastic spheres in contact

E. Dintwa[a], M. van Zeebroeck, E. Tijskens[b], and H. Ramon

Laboratorium Landbouwwerktuigkunde, K.U. Leuven, Kasteelpark Arenberg 30, 3001, Leuven, Belgium

Received 15 November 2003 / Received in final form 6 January 2004
Published online 18 June 2004 –

Abstract. The theory of elastic contact between two spherical bodies according to Hertz, Mindlin and others is used as a basis for an extension to include the contribution of the viscous effects to the total stress for viscoelastic spheres subjected to twisting moments. Expressions relating twisting moment to the radius of a 'stick' region of the contact surface and the radius of the 'stick' region to twist angle are derived. Two term power series truncations of the relations are then used to derive approximate expressions for torsional stiffness of the bodies. Validation of the model was by experiments utilising a rheometer device. Applications for the model in post-harvest agriculture include extraction of material surface properties for use in discrete element modelling of mechanical interactions of fruits and other spheroidal produce during machine handling.

PACS. 46.35.+z Viscoelasticity, plasticity, viscoplasticity – 46.55.+d Tribology and mechanical contacts – 62.20.Dc Elasticity, elastic constants

1 Introduction

Granular materials are abundant in nature and nearly, if not, in all sectors of industry. The agro-industry, with nearly every harvested product going through at least one granular stage in the handling chain from harvest to consumption, is not an exception. A deep understanding of the motion of the 'grains' and the intensities of impact forces endured by the material over time during various handling processes is necessary if improvements are to be made to the handling systems or equipment. On the level of one impact, there exist several experimental techniques (such as pendulum experiments, puncture tests and UTS tests) to study the mechanical relationships between the forces involved and the resulting material deformations. At the level of a whole mechanised process, however, it becomes impractical to experimentally track all the individual granular units in the system and record all their interactions with other individuals and machine parts as a function of space and time. Mathematical models provide the obvious alternative for gaining this required understanding of the various mechanical interactions involved in such processes.

Mechanical interactions between non-conforming bodies will invariably involve normal contact in combination with relative contact surface motions such as sliding, spinning or rolling. A substantial amount of work was done, particularly in the 50's, with regard to the solution of the problem of normal contact of non-conforming objects [1–5]. Extensions on the problem have been performed to cover more scenarios such as combined normal and translational tangential forces [2,6], torsional forces [2,7,8] and rolling resistance [5,9]. The models generated in these works provide sufficient description for the contact interactions of elastic bodies. However, a great portion of materials cannot be rated elastic even at small strains, making it necessary for the above results to be extended to cover such materials. Such extensions have been made to describe elastoplastic [10–13] as well as viscoelastic materials [14–21]. For viscoelastic spheres, the extensions have been made to describe normal collisions [14–17] and rolling [18–21] while little has been achieved to cover sliding and spinning contact.

In the framework of continuum mechanics, the correct mathematical formulation of a contact problem consists of a system of partial differential equations expressing conservation of mass, momentum and energy, supplemented with constitutive equations describing the material behaviour. Solving these equations leads to the displacements and stresses as a function of space and time. The finite element (FE) method is appropriate in performing this analysis and it can be complimented with experiment for verification. Shih et al. [22] provided experimental and FE verification of the stress distributions that are predicted by Hertz's theory for normal contact of elastic spheres while Vu-Quoc et al. [23] presented a FE validation for both Hertz's theory and that of Mindlin and Deresiewicz [6] for oblique contact of elastic spheres.

[a] e-mail: Edward.Dintwa@agr.kuleuven.ac.be
[b] e-mail: Engelbert.Tijskens@agr.kuleuven.ac.be

From the foregoing, it is apparent that there exist three options to determine contact force-deformation relations for a single contact situation namely: theoretical models, experiment and FE models. Considering a whole process, it has already been mentioned that the experimental methods become impractical in providing spatio-temporal records of all the collisions amongst individuals. The FE approach is also only routinely applicable on the scale of a single impact problem. On the scale of an entire process far too many impacts are occurring simultaneously to be computationally tractable in this way, therefore a computationally simpler method is required. In this regard, the discrete element method (DEM) has recently emerged [13,24,25] as the most promising modelling technique for agricultural processes.

The DEM is essentially a numerical technique to model a system of particles interacting with one another and with the system boundaries through collisions [24,26]. Equations of motion are numerically integrated in time to obtain velocities and location at the next time step. In this way, the technique describes the path of every particle in the system in time and records the collision history of the particle. In a DEM model, instead of the material constitutive equations, contact force laws are used to approximate the collision process. For each pair of objects in contact, the contact laws represent the behaviour simply as a single deformation vector and a point force rather than the displacements and stresses. The deformation vector and contact force can be decomposed into normal and tangential or torsional components. A separate contact force model describes each component. The normal contact force model relates the normal component of the deformation vector to the normal component of the contact force, and the tangential and torsional contact force models relate the tangential and torsional components of the deformation vector to the respective tangential and torsional components of the contact force. Contact force models hold the key to accurate DEM simulations. They are required to be as simple as possible to limit computational complexity while providing an accurate estimation of the force-deformation relationship. For a majority of DEM applications and for agricultural produce in particular, simple but accurate contact force models are a challenge that needs urgent attention to allow achievement of the desired accuracy of the DEM models. Generally, the contact models can be developed through any (or combination any) of the three methods mentioned above: theoretical models, experiment or FE models.

Agricultural materials possess time-dependent force-deformation responses and are considered to be viscoelastic [27–33]. An experimental procedure to determine the parameters of a normal contact force model for fruits is described by van Zeebroeck et al. [25]. This paper focuses on the spinning or twisting action of two viscoelastic spheres in contact and describes a derivation of a torsional contact force model for the spheres. The model is to be applied in experimental work to determine the parameters of a tangential contact force model (i.e. friction coefficient, shear modulus, shear viscosity) for incorporation into a DEM model for agricultural produce (fruits and vegetables). Validation of the model is performed with experiments utilising a rheometer device and a direct application of the derived model is demonstrated through experiments to determine the friction coefficients of whole fruits, using a rheometer device.

2 Torsion of elastic spheres in contact

For a system of two elastic spheres in contact, the cylindrical coordinate system with the origin at the centre of the contact surface and the z-axis passing through the centroids of both spheres is adopted. We define the displacements u_r, u_θ and u_z in the r, θ and z directions respectively. The material is assumed to be linearly elastic and the deformations are assumed to be small (infinitesimal strain). Under these conditions, the response of two contacting spheres subjected to combined normal and torsional forces is equivalent to the case of normal loading followed by torsion [2,35]. At the contact surface, the normal contact force causes displacements only in the normal direction (only u_z), with all the other components of displacement being zero. On the other hand, it has been shown, through symmetry considerations [2], that u_θ is the only non-zero component that arises at the contact surface due to the action of a twisting moment on the already normally loaded system. Consequently, it can be concluded that there is no coupling between the actions of the normal contact force and the twisting couple and that they can be analysed separately. It might be important to clarify that this does not imply that the two loads are physically independent (in this respect, it should be easy to see that the torsional part cannot exist without the normal part since this would imply no contact between the spheres). However, the stresses and strains resulting from the load components are independent and therefore can be analysed independently. Hence, a solution for the stresses and strains arising from torsional loading of spheres in contact can be decomposed into the two parts: the first part for the normal component of the loading and the second for the torsional component. The total stress is a superposition of the stresses that arise from both.

The solution for normal contact follows from the Hertz theory [1], results of which are summarized as follows: under the action of a normal force P, a flat circular contact surface of radius a results. The pressure distribution p over the contact area is given by

$$p = p_0 \left\{1 - \left(r^2/a^2\right)\right\}^{1/2} \tag{1}$$

where p_0 is the average normal pressure across the area i.e. $p_0 = 3P/(2\pi a^2)$ and r is the radial distance from the centre of the contact surface and on the plane of the contact surface. The contact radius is given by:

$$a = \left(\frac{3PR}{4E^*}\right)^{1/2} \tag{2}$$

where the constant E^* represents the elastic properties of the two materials in contact:

$$\frac{1}{E^*} = \frac{1-\nu_1^2}{E_1} + \frac{1-\nu_2^2}{E_2}$$
$$(E_1,\ E_2 = \text{Young}'\text{s moduli},\ \nu_1,\ \nu_2 = \text{Poisson}'\text{s ratios}) \quad (3)$$

and R is the relative radius of the bodies ($1/R = 1/R_1 + 1/R_2$; R_1 and R_2 are the radii for body one and two respectively). Lastly, the relative approach of the centroids of the spheres (or total deflection) δ, is given by:

$$\delta = \left(\frac{9P^2}{16RE^{*2}}\right)^{1/3}. \quad (4)$$

The above results apply for linear elastic materials undergoing infinitesimal strain. The above theory also assumes a flat contact interface. For spheres of different elasticity moduli, this could be a source of error as the contact surface is generally not flat. Rather, the stiffer body will dome into the less stiff one.

If, in addition to the normal loading, a twisting moment M_z is applied about the axis of normal contact, the contact surface will undergo some rotation (relative to a distant point within each body) by a twist angle β. The friction force at the contact surface will provide resistance to sliding. The condition for slip at any point within the contact surface is according to the Amontons'-Coulomb law, and can be stated as follows:

$$|q| \le \mu|p| \qquad \text{- no slip}$$
$$|q| > \mu|p| \qquad \text{- slip}$$

where q is the traction in a tangential direction. For contacting elastic spheres, the torsional shear traction that develops at the contact surface is a function of r (i.e. $q(r)$) and it goes to infinity as r approaches a [2]. Slip will therefore inevitably occur at the boundary of the contact surface regardless of how small the twisting moment M_z is. Slip starts at the edge of the surface and develops radially inwards on an annulus as the twisting moment is increased. Across the slip annulus the traction assumes the limiting value i.e. $q(r) = \mu p(r)$; $c \le r \le a$, where c is the radius of the stick region of the contact surface and $p(r)$ arises from the Hertz pressure distribution (Eq. (1)).

The co-existence of a slip region and 'stick' region within the contact surface presents a mixed boundary value problem in elasticity. The boundary conditions are stated as:

$$\mu_\theta = \beta r,\ \mu_r = \sigma_z = 0; \qquad r \le c,\ z = 0$$
$$\tau_{z\theta} = q(r) = \frac{3\mu P}{2\pi a^3}\sqrt{a^2 - r^2}; \quad \tau_{rz} = \sigma_z = 0; \qquad c \le r \le a,\ z = 0 \quad (5)$$

where σ_z, $\tau_{z\theta}$, τ_{rz} are the additional stress components arising from the moment load component. Solution of this problem [7] yields the elastic torsional shear stress that develops on the contact surface ($z = 0$):

$$\tau^e_{z\theta} = q(r) = \frac{3\mu P}{2\pi(a)^2}\left(1 - \frac{r^2}{a^2}\right)^{1/2}, \quad c \le r \le a$$
$$\tau^e_{z\theta} = q(r) = \frac{3\mu P}{(\pi a)^2}\left(1 - \frac{r^2}{a^2}\right)^{1/2} \times \left[\frac{\pi}{2} + k^2 D(k)F(k',\varphi) - K(k)E(k',\varphi)\right], \quad r \le c \quad (6)$$

where;

$$k = \sqrt{1-(c/a)^2} = \sqrt{1-k'^2}; \quad (7)$$
$$k' = \frac{c}{a}; \quad (8)$$
$$\varphi = \sin^{-1}\frac{1}{k'}\sqrt{\frac{k'^2 - (r/a)^2}{1-(r/a)^2}}; \quad (9)$$

$F(k',\varphi)$, $E(k',\varphi)$ are the elliptical integrals of the first and second kind respectively, with modulus k' and amplitude φ [36].

$D(k)$ is the complete elliptical integral with modulus k, given by $D(k) = (K-E)/k^2$ with K and E being complete elliptical integrals of the first and second type (modulus k) respectively.

It can be verified that when $r = c$, the two versions of equation yield the same value hence confirming the continuity of the shear stress $\tau^e_{z\theta}$ at c.

The relationship between the twist angle β and the radius c is given by

$$\beta = \frac{3\mu P}{4\pi G a^2}k^2 D(k) \quad (10)$$

where k is related to c according to equation (7). The relationship between the applied moment and the radius of the stick region is found from the condition of equilibrium

$$M_z = 2\pi\int_0^a q(r)r^2 dr, \quad (11)$$

yielding the expression for the elastic twisting moment M^e_z:

$$M^e_z = \frac{\mu P a}{4\pi}\left\{\frac{3\pi^2}{4} + k'k^2\left[6K(k) + \left(4k'^2 - 3\right)D\right] - 3kK(k)\sin^{-1}k' - 3k^2\left[K(k)\int_0^{\pi/2}\frac{\sin^{-1}(k'\sin\alpha)d\alpha}{(1-k'^2\sin^2\alpha)^{3/2}} - D(k)\int_0^{\pi/2}\frac{\sin^{-1}(k'\sin\alpha)d\alpha}{(1-k'^2\sin^2\alpha)^{1/2}}\right]\right\}. \quad (12)$$

As the twisting moment is increased the stick region shrinks until at the onset of free sliding when the stick region has been reduced to a point at the centre. The value

of twisting moment necessary to initiate the free sliding is given by:

$$M_z^e(max) = \frac{3\pi}{16}\mu Pa. \tag{13}$$

Deresiewicz [35] derived explicit approximate relations between the three quantities (stick radius c, twisting moment M_z^e and twist angle β) by using two-term power series expansions of the exact relations above. The relations are only applicable for small values of twisting moment ($M_z^e/\mu Pa \ll 1$ or $k' = c/a \approx 1$) and are as follows:

$$\frac{M_z^e}{\mu Pa} = \frac{2}{3}\left[1 - \frac{1}{6}\left(1 + 3\left(\frac{a}{c}\right)^2\right)^2\right] \tag{14}$$

$$\frac{c}{a} = \frac{1}{\sqrt{3}}\sqrt{4\left(1 - \frac{3}{2}\frac{M_z^e}{\mu Pa}\right)^{1/2} - 1} \tag{15}$$

$$\frac{Ga^2\beta}{\mu P} = \frac{3}{128}\left(1 - \frac{c^2}{a^2}\right)\left(11 - 3\frac{c^2}{a^2}\right). \tag{16}$$

Substituting equation (15) into (16) an explicit moment-twist relation was determined as:

$$\frac{Ga^2\beta}{\mu P} = \frac{1}{8}\left[1 - \left(1 - \frac{3}{2}\frac{M_z^e}{\mu Pa}\right)^{1/2}\right]\left[3 - \left(1 - \frac{3}{2}\frac{M_z^e}{\mu Pa}\right)\right] \tag{17}$$

leading to a torsional compliance

$$C_t^e \equiv \frac{d\beta}{dM_z^e} = \frac{3}{16a^3G}\left[2\left(1 - \frac{3}{2}\frac{M_z^e}{\mu Pa}\right)^{-1/2} - 1\right]. \tag{18}$$

3 Viscous component

In deriving the solutions for the elastic problem, the material constitutive law is taken as Hooke's law, which for isotropic materials reads:

$$\sigma_{ij}^e = \lambda e_{\alpha\alpha}\delta_{ij} + 2\eta e_{ij} \tag{19}$$

where: σ^e, e are the stress and strain tensors, δ is the Kronecker delta, λ, η are Lamé's constants and they are related to the Young's modulus E, shear modulus G and Poisson's ratio ν.

For viscous flow, an analogous constitutive law applies for an isotropic Newtonian fluid and it reads

$$\sigma_{ij}^\nu = \lambda_\nu \dot{e}_{\alpha\alpha}\delta_{ij} + 2\eta_\nu \dot{e}_{ij} \tag{20}$$

when neglecting static pressure [37]. σ^ν is the viscous stress tensor and $\dot{e}$ is the strain rate tensor, which is essentially the same as the strain tensor in the elasticity law but with the deformations replaced by deformation rates.

If the total stress on the bodies is taken as a sum of the elastic component and viscous component of the deformation process, the following can be written for the total stress

$$\sigma_{ij} = \sigma_{ij}^e + \sigma_{ij}^\nu = \lambda e_{\alpha\alpha}\delta_{ij} + 2\eta e_{ij} + \lambda_\nu \dot{e}_{\alpha\alpha}\delta_{ij} + 2\eta_\nu \dot{e}_i. \tag{21}$$

It is worth noting that the forgoing is not meant to imply that the force-deformation process is easily decomposable into the pure viscous and pure elastic components in parallel (i.e. Voigt model type). On the contrary, a real viscoelastic material will behave like a complex mixture of elastic and viscous elements interconnected both in parallel and in series as commonly modelled by complex rheological spring-dashpot models such as the generalized Maxwell or Voigt models.

As discussed earlier (Sect. 2), a solution for the stresses and strains arising from torsional loading of spheres in contact can be decomposed into the normal force component and the torsional moment component, with the total solution being a superposition of the two. The subject of the normal contact of viscoelastic spheres has already been extensively covered [15–17]. In this article, only the twisting action of viscoelastic spheres already subjected to normal contact force is considered. Considering the twisting action, the traction distribution at the contact surface arising from a moment M_z is given by the shear stress $\tau_{z\theta}$ on the contact surface. From equation (21), the shear stress component $\tau_{z\theta}$ is given by:

$$\tau_{z\theta} = 2(\eta e_{z\theta} + \eta_\nu \dot{e}\theta). \tag{22}$$

If infinitesimal strain and strain rate are assumed, then the shear strain and strain rate, in cylindrical coordinates, are given by:

$$e_{z\theta} = \frac{1}{2}\left(\frac{1}{r}\frac{\partial u_z}{\partial \theta} + \frac{\partial u_\theta}{\partial z}\right); \quad \dot{e}_{z\theta} = \frac{1}{2}\left(\frac{1}{r}\frac{\partial \dot{u}_z}{\partial \theta} + \frac{\partial \dot{u}_\theta}{\partial z}\right) \tag{23}$$

and since a flat contact surface is assumed (i.e. $\partial u_\theta/\partial z = 0$), it follows that the total shear stress for a viscoelastic material is given by:

$$\tau_{z\theta} = \eta\frac{\partial u_\theta}{\partial z} + \eta_\nu\frac{\partial \dot{u}_\theta}{\partial z}. \tag{24}$$

The constants η and η_ν are the modulus of rigidity (normally denoted G) and the viscosity of the material respectively.

Notably, the viscous stress constitutive law for an isotropic Newtonian fluid (Eq. (20)) is equivalent to Hooke's law for an isotropic solid (Eq. (19)) but with the elastic constants (λ, η) replaced by the viscous constants (λ_ν, η_ν) respectively and the strain tensors replaced by the strain rate tensors. The viscous stress component is assumed to follow the same distribution in the body as the elastic stress component. It will be appreciated that, in strict terms, this is true only in the absence of the elastic stress component due to the dependence of the viscous component on the later. Nevertheless this assumption is necessary to simplify further analysis.

An important property of the solution for the elastic contact problem is that the displacement fields $u_\theta(r)$ are fully determined by the twisting moment M_z^e and thus by the twist angle β. Therefore we can write $u_\theta(r) = u_\theta(r, \beta)$, to indicate that the displacement field depends parametrically on the twist angle. The displacement velocities in

the quasi-static approximation [16,38] can then be obtained as:

$$\dot{u}_\theta(r,t) = \dot{\beta}\frac{\partial u_\theta(r,\beta)}{\partial\beta}. \tag{25}$$

Thus, the dissipative component of the stress in equation (24) can be written as

$$\tau^\nu_{z\theta} = \dot{\beta}\frac{\partial}{\partial\beta}\left[\eta_\nu\frac{\partial u_\theta}{\partial z}\right] = \dot{\beta}\frac{\partial}{\partial\beta}\tau^e_{z\theta}(\eta\to\eta_\nu) \tag{26}$$

where the expression in parenthesis indicates that the expression in the square brackets is the same as the elastic stress but with the elastic constant replaced by the viscous constant.

If we introduce a parameter α such that $\alpha = \eta_\nu/\eta$, then the shear stress on the contact surface can be expressed as

$$\tau^\nu_{z\theta}(r,\theta,0) = \alpha\dot{\beta}\frac{\partial}{\partial\beta}\left[\tau^e_{z\theta}(r,\theta,0)\right]. \tag{27}$$

Recalling the expression for the elastic torsional shear traction distribution presented in equation (6) and noting that at the contact surface the rate of change of the twist angle $\dot{\beta}$ equals the angular velocity ω of the twisting action, the forgoing can be written as follows:

$$\tau^\nu_{z\theta}(r,\theta,0) = \alpha\omega\frac{\partial}{\partial\beta}\left[\frac{3\mu P}{(\pi a)^2}\left(1-\frac{r^2}{a^2}\right)^{1/2} \times\left(\frac{\pi}{2}+k^2D(k)F(k',\varphi)-K(k)E(k',\varphi)\right)\right]. \tag{28}$$

The total viscous moment may be obtained by integrating the viscous stress over the contact area to get:

$$M^\nu_z = \alpha\omega\frac{\partial}{\partial\beta}M^e_z \tag{29}$$

which gives a simple expression for the viscous contribution to the total twist moment for viscoelastic objects as a function of the elastic moment and dependent on the angular velocity ω as well as the ratio α of the material viscosity to the material shear modulus. The expression for M^e_z is given by equation (12). The differential in this equation can be recognised as the elastic (or static) torsional stiffness S^e of the contacting spheres (i.e. inverse of the elastic compliance C^e_t in Eq. (18)), expressions of which can be recalled from the previous section. Therefore, the above suggests that the viscous contribution is determined as a simple product of the ratio of the material viscosity to the material elastic shear modulus, the angular velocity of the twisting action and the system elastic stiffness. The full expression for the viscous contribution to the twist moment can be written

$$M^\nu_z = \frac{\eta_\nu\omega\mu Pa}{4\pi G}\frac{\partial}{\partial\beta}\left\{\frac{3\pi^2}{4}+k'k^2\left[6K(k)+(4k'^2-3)D\right] - 3kK(k)\arcsin k' - 3k^2\left[K(k)\int_0^{\pi/2}\frac{\sin^{-1}(k'\sin\alpha)\,d\alpha}{\left(1-k'^2\sin^2\alpha\right)^{3/2}} - D(k)\int_0^{\pi/2}\frac{\sin^{-1}(k'\sin\alpha)d\alpha}{(1-k'^2\sin^2\alpha)^{1/2}}\right]\right\}. \tag{30}$$

It is easy to note that during free sliding, there is no viscous contribution to the twist moment resistance because from that point on the elastic contribution to twist moment remains constant [equation] for any further increase in the twist angle (i.e. $\partial M^e_z/\partial\beta = 0$).

If we now use the approximate moment-twist angle relationship as per equation (17), we can write an expression for the viscous moment as

$$M^\nu_z = \frac{16a^3\eta_\nu\omega}{3\left[2\left(1-\frac{3}{2}\frac{M^e_z}{\mu Pa}\right)^{-1/2}-1\right]}. \tag{31}$$

4 Total torsional friction for a viscoelastic sphere

The torsion problem for a viscoelastic sphere can now be expressed. The surface ($z = 0$) tractions are:

$$\tau_{z\theta} = \frac{3\mu P}{2\pi a^3}\sqrt{a^2-r^2}, \quad c\le r\le a$$

$$\tau_{z\theta} = \left(1+\alpha\omega\frac{\partial}{\partial\beta}\right)\frac{3\mu P}{(\pi a)^2}\left\{\left(1-\frac{r^2}{a^2}\right)^{1/2} \times\left[\frac{\pi}{2}+k^2D(k)F(k',\varphi)-K(k)E(k',\varphi)\right]\right\}, \quad r\le c$$

$$\tau_{rz} = 0 = \sigma_z = 0. \tag{32}$$

The relationship between the stick radius and the twist angle is given by equation (10) and the total twisting moment is given by

$$M_z = M^e_z + M^\nu_z = M^e_z + \frac{\eta_\nu\omega}{G}\frac{\partial M^e_z}{\partial\beta} \tag{33}$$

which, from equation (12) becomes

$$M_z = \frac{\mu Pa}{4\pi}\left(1+\frac{\eta_\nu\omega}{G}\frac{\partial}{\partial\beta}\right) \times\left\{\frac{3\pi^2}{4}+k'k^2\left[6K(k)+\left(4k'^2-3\right)D\right]-3kK(k)\sin^{-1}k' - 3k^2\left[K(k)\int_0^{\pi/2}\frac{\sin^{-1}(k'\sin\alpha)d\alpha}{\left(1-k'^2\sin^2\alpha\right)^{3/2}} - D(k)\int_0^{\pi/2}\frac{\sin^{-1}(k'\sin\alpha)d\alpha}{\left(1-k'^2\sin^2\alpha\right)^{1/2}}\right]\right\}. \tag{34}$$

The limiting torsional moment at steady state free sliding is given by equation (13).

Figure 1 shows the typical moment-twist profile that results from equation (34) when the twist is performed at two different constant angular velocities for the same viscoelastic sphere. Compared to the model without the viscous element it can clearly be seen from the graph that an additional torque is required to produce the same twist angle when the object has viscous resistance. Higher angular

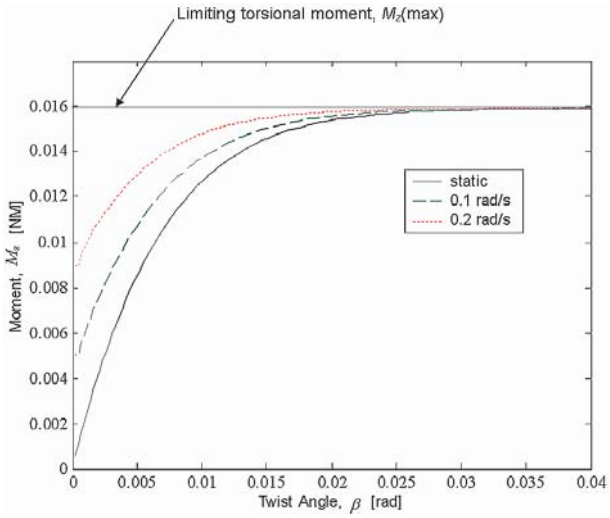

Fig. 1. Typical moment-twist angle profiles of a viscoelastic sphere twisted at two different speeds (0.1 rad/s and 0.2 rad/s) compared to the profile for static twisting [normal force $P =$ 20 N, contact radius $a = 5$ mm, viscosity $\eta_\nu = 6500$ Pa s, friction coefficient $\mu = 0.27$].

velocities result in higher viscous resistance contributions and thus higher torques necessary to produce the same twist angles. The viscous resistance contribution gradually reduces as the twist angle increases due to the diminishing of the elastic stiffness.

From equations (14–16) and with M_z^ν given by equation (31) the following approximate relations for very small twist angles can be written:

$$M_z = M_z^e + \frac{16a^3\eta_\nu\omega}{3\left[2\left(1-\frac{3}{2}\frac{M_z^e}{\mu Pa}\right)^{-1/2}-1\right]} \tag{35}$$

with M_z^e given by equation (14) or (15). Combining this equation with equation (16) will lead to an explicit approximate equation for the moment-twist relationship for viscoelastic spheres. The apparent stiffness S of the twisting process can be written as

$$S = \frac{dM_z}{d\beta} = \frac{dM_z^e}{d\beta} + \frac{dM_z^\nu}{d\beta} = \frac{dM_z^e}{d\beta} + \frac{\eta_\nu\omega}{G}\frac{d^2M_z^e}{d\beta^2} \tag{36}$$

and completing the differentiation we obtain

$$S = S^e\left\{1 - \frac{9\eta_\nu\omega}{32\mu G^2Pa^4}\left(1-\frac{3M_z^e}{2\mu Pa}\right)(S^e)^2\right\} \tag{37}$$

where the elastic stiffness S^e is the elastic torsional stiffness of the contacting spheres. The inverse of S gives the compliance of the system. As can be seen, when either the viscosity η_ν or the angular velocity ω is zero, the expression for the compliance reverts to equation (18).

5 Model validation and experimental results

Two sets of experiments were performed for the purpose of validating the model as described. The first set was for the validation of the model for static torsion (i.e. very low angular velocities) while the second set was for dynamic torsion. Further, as a direct application of the model, some experiments were performed to determine the dynamic friction coefficient of whole fruit. All the experiments were performed by use of a rheometer device (AR 1000 N, TA Instruments, USA).

In the experimental set-up, two fruits, one fixed to the rheometer shaft and the other to the stationary base, were placed in contact and subjected to a prescribed normal force. A tactile membrane (I-scan 5051, Tekscan, MA, USA) sandwiched between the contacting spheres was used to measure the contact radius. The rheometer exerts a prescribed twisting moment via the rheometer shaft while recording data on the applied moment, angular displacement and angular velocity. Apple (Jonagold) fruits were used for all the validation experiments. A further description of the experiments can be found in van Zeebroeck et al. [34].

5.1 Static validation

For the purpose of validating the model for static moments, the two contacting fruits were subjected to static torsion. To achieve this regime with the rheometer, a continuous ramp (of the applied moment over time) operation mode was adopted. In this mode, the moment was steadily increased from zero to the prescribed maximum. By choosing very long times to reach the prescribed moment, very low angular velocities could be achieved. Under this regime the moment-twist relationship for the fruits is described by equation (12).

Figure 2 shows a typical plot of torque *vs.* angular displacement for an apple fruit. As can be clearly seen from the plot, the model (theoretical curve) gives a satisfactory prediction of the moment-twist profile. To eliminate prediction error caused by parameter variability a computer optimised set of model parameters was used with the model (giving the optimised theoretical curve in the figure) rather than the previously measured material parameters (non-optimised curve in the figure). The parameter optimisation technique involved selective variation of the individual model parameters, within their measured variability range (or accuracy ranges of the measuring methods), and selecting the parameter combination that results in the least error sum of squares (ESS) between the model and the experiment. The model parameters involved for the static validation experiment are the friction coefficient μ, the modulus of rigidity G, and the contact surface area a.

5.2 Dynamic validation

For the validation of the model for dynamic torsion, a regime involving comparatively large angular velocities was chosen. High angular velocities could be achieved using the oscillation mode of the rheometer. In this program, sinusoidal twist moment is applied to the contacting

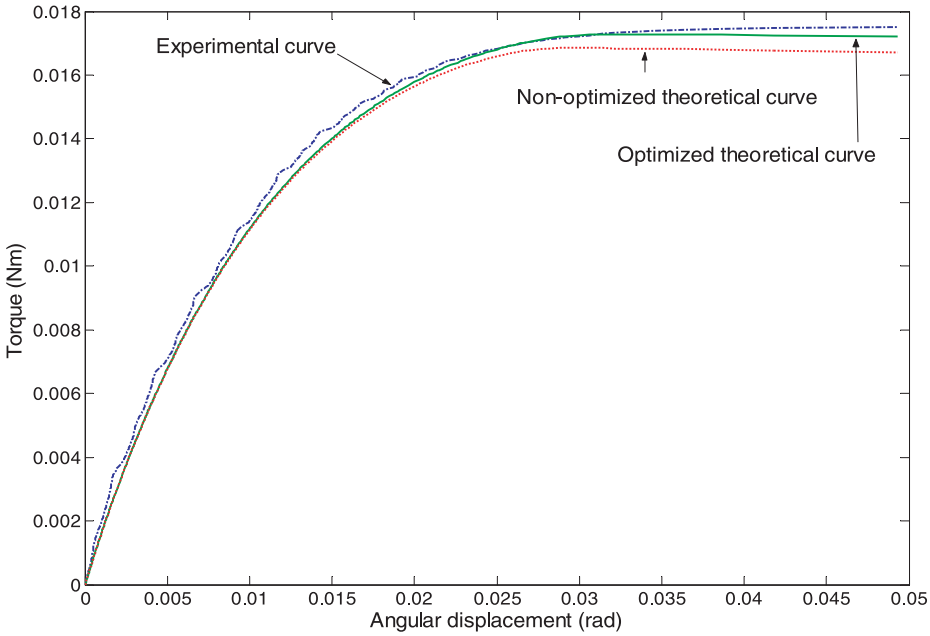

Fig. 2. Typical torque vs. angular displacement curve for static torsion of an apple in contact with another apple (shear modulus $G = 3.39$ MPa, viscosity $\eta_\nu = 5906$ Pa s, friction coefficient $\mu = 0.31$, normal force $P = 19.32$ N, contact radius $a = 0.0056$ m).

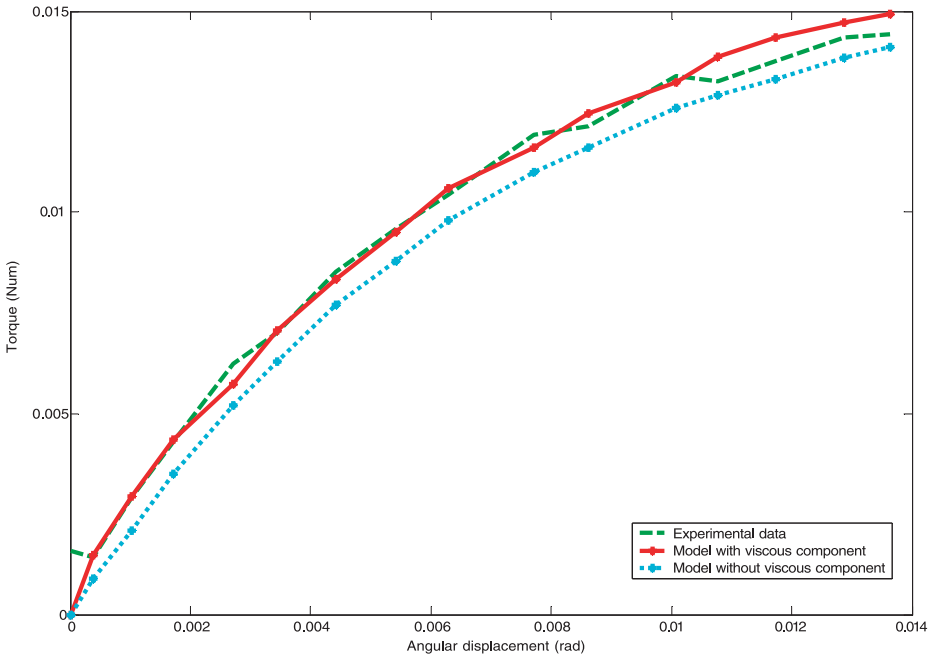

Fig. 3. Plot of torque vs. angular displacement for an apple subjected to dynamic torsion showing the measured curve, theoretical curves according to the viscoelastic sphere model and elastic sphere model (shear modulus $G = 3.42$ MPa, viscosity $\eta_\nu = 6658$ Pa s, friction coefficient $\mu = 0.27$, normal force $P = 20.05$ N, contact radius $a = 0.005$ m.

objects at a prescribed frequency and torque amplitude. The torque amplitude was chosen to ensure complete sliding between the fruits while higher velocities could be achieved by increasing the frequency. Only a curve representing a quarter of an oscillation period (torque increasing from zero to positive amplitude) was taken for comparison with the model. The theoretical curve is calculated from the model using equation (36).

Figure 3 shows typical plots of the torque vs. angular displacement. In the figure the measured curve is compared to the calculated curves according to both the new viscoelastic model and the elastic model. From the figure it can clearly be seen that the profile calculated using the derived model for a viscoelastic sphere gives a remarkably better prediction of the experimental profile compared to the elastic sphere model. Hence, it can be

concluded that the new proposed model is valid for describing the moment-twist profile of viscoelastic spheres and that it offers improved prediction of the dynamic moment-twist profile for viscoelastic spheres in contact.

5.3 Determination of the dynamic friction coefficient

The described set up was also used for the determination of the dynamic friction coefficient μ for two contacting fruits. In these experiments, a steadily increasing moment was applied onto the rotating fruit until complete sliding between the contact surfaces occurred. The formula giving the torque during complete sliding (Eq. (13)) was then used to determine the friction coefficient μ. To determine μ for interfaces of the fruit with other surfaces (i.e. metal), the bottom fixed fruit was replaced with a flat plate of the metal under investigation. From these experiments, the friction coefficient for apple-apple contact was determined as 0.27 ± 0.08 while that for the apple-aluminium contact was 0.27 ± 0.03. The friction coefficient value for the apple-aluminium contact is in agreement with the value for steel-apple contact found in literature [27]). No relevant data could be found in literature for the apple-apple contact.

In general, friction coefficient data for fruit-fruit contacts are rarely obtainable from literature. This is probably due to the fact that, traditionally, very complex experimental set-ups are necessary to obtain these. The rheometer method therefore alleviates the problem by providing an easy set up that takes advantage of the high precision sensors and the efficient data acquisition systems that come with rheometers

6 Discussion and conclusions

The twisting action of two viscoelastic spheres in contact was treated. Results from past treatments of the problem of the twisting action between two elastic spheres in contact were first presented. To these, extensions were made to incorporate the viscous dissipative nature of viscoelastic materials. The extension is based on the assumption that the stress within the bodies can be represented by a sum of a pure elastic component and a pure viscous component. It is argued that, especially for Discrete Element Method (DEM) modelling applications, while this is a drastic simplification, it will provide a good approximation of the force-deformation behaviour if combined with accurate experimental data for the material properties.

From the above, models were developed giving the relationship between the twist angle and the radius of the stick region of the contact surface as well as that between the twisting moment and the twist angle. Explicit approximate relations between each pair of the three quantities (stick radius, twisting moment and twist angle) were obtained for small twisting moments leading to an approximate expression for the torsional compliance of a viscoelastic sphere.

The treatment is limited to objects that form the Hertzian flat contact surface (e.g. contact between spheres of the same material or contact between a sphere and a flat surfaced body with the sphere being of a softer material). Also, it was performed for viscoelastic spheres undergoing only the basic actions of normal force followed by a twisting moment. Extensions to describe the more realistic scenarios such as simultaneous increment/reduction of both pressure and twist or oscillatory twisting actions are possible by representing the force deformation profile as a cumulative effect of small increments (or reductions) in the normal force followed by small increments in the twisting moment [6,35]. Generalisation to non-conforming objects of various shapes is necessary to treat less regular objects. Finally, the above models are applicable under conditions of quasi-static collisions (dissipation due to attenuation of vibrations neglected) and small strains. Quasi-static approximation is valid when the characteristic relative velocity of the objects in contact is much less than the speed of sound in the material. In the case of viscoelastic materials, as shown by Brilliantov et al. [38], there is an additional condition that the duration of a collision (or any other contact process) should be much larger than the material relaxation time for the quasi-static approximation to be valid. The experiments reported on herein satisfy these conditions comfortably.

The developed models would be useful in any application where spinning contacts of spheroidal viscoelastic objects are a significant mode of system interactions. For postharvest applications, the model could be useful in experiments to determine the salient parameters of contact-force models for fruits (i.e. friction coefficient, viscosity, shear modulus). In this regard, the possible use of the model in experiments to determine the coefficients of friction in fruit-fruit contacts was demonstrated. Contact force models are crucial elements for DEM models of particle systems. There is ongoing work to model fruit-handling operations such as machine harvesting and transportation in conveyor belts and trucks by the DEM [24]. Such models, when coupled with bruise or damage prediction models, are capable of predicting the amount of damage that can occur to fruits during respective unit operations. This information would be useful in designing and optimising fruit handling systems to minimise fruit damage.

The authors acknowledge the financial support of the Fonds voor Wetenschappelyk Onderzoek (FWO), the Instituut voor de aanmoediging van innovatie door Wetenschap en Technologie in Vlaanderen (IWT-Vlaanderen), and the K.U. Leuven Research Fund.

References

1. H. Hertz, J. Reine Angew. Math. **94**, 156 (1882); English translation in Miscellaneous Papers by H. Hertz (Eds. Jones and Schott, London, Macmillan, 1896)
2. R.D. Mindlin, ASME J. Appl. Mech. **16**, 259 (1949)
3. S. Timoshenko, J.N. Goodier, *Theory of Elasticity*, 2nd edn. (McGraw-Hill, New York, 1951)

4. A.E.H. Love, *A Treatise on the Mathematical Theory of Elasticity*, 4th edn. (Cambridge University Press, New York, 1952)
5. K.L. Johnson, *Contact Mechanics*, 2nd edn. (Cambridge University Press, New York, 1985)
6. R.D. Mindlin, H. Deresiewicz, ASME J. Appl. Mech. **20**, 327 (1953)
7. J.L. Lubkin, ASME J. Appl. Mech. **18**, 183 (1951)
8. M. Hetenyi, J.R. McDonald, ASME J. Appl. Mech. **25**, 396 (1958)
9. J.P. Bardet, Q. Huang, in *Proceedings of the Second International Conference on Micromechanics of Granular Media*, 1993, edited by C. Thornton (A.A. Balkema, Rotterdam, The Netherlands, 1993), p. 39
10. O.R. Walton, R.L. Braun, J. Rheol. **30**, 949 (1986)
11. C. Thornton, ASME J. Appl. Mech. **64**, 383 (1997)
12. X. Zhang, L. Vu-Quoc, Mech. Mater. **31**, 235 (1999)
13. L. Vu-Quoc, X. Xhang, L. Lesburg, ASME J. Appl. Mech. **67**, 363 (2000)
14. E.H. Lee, J.R.M. Radock, ASME J. Appl. Mech. **27**, 438 (1960)
15. G. Kuwabara, K. Kono, Jap. J. Appl. Phys. **26**, 1230 (1987)
16. J.M. Hertzsch, F. Spahn, N.V. Brilliantov, J. Phys. II France **5**, 1725 (1995)
17. R. Ramírez, T. Pöschel, N.V. Brilliantov, T. Schwager, Phys. Rev. E **60**, 4465 (1999)
18. K. Iwashita, M. Oda, ASCE J. Engrg. Mech. **124**, 285 (1998)
19. N.V. Brilliantov, T. Pöschel, Europhys. Lett. **42**, 511 (1998)
20. N.V. Brilliantov, T. Pöschel, Eur. Phys. J. B **12**, 299 (1999)
21. T. Pöschel, T. Schwager, N.V. Brilliantov, Eur. Phys. J. B **10**, 169 (1999)
22. C.W. Shih, W.S. Schlein, J.C.M. Li, J. Mat. Res. **7**, 1011 (1992)
23. L. Vu-Quoc, X.G. Zhang, L. Lesburg, Int. J. Solids Struct. **38**, 6455 (2001)
24. E. Tijskens, H. Ramon, J. De Baerdemaeker, J. Sound Vib. **266**, 493 (2003)
25. M. van Zeebroeck, E. Tijskens, P. van Liedekerke, V. Deli, J. De Baerdemaeker, H. Ramon, J. Sound Vib. **266**, 465 (2003)
26. P. Cundall, O. Strak, Geotech. **29**, 47 (1979)
27. D.D. Hamann, Trans. ASAE **13**, 893 (1970)
28. P. Chen, R.B. Fridley, Trans. ASAE **15**, 1103 (1972)
29. J.G. De Baerdemaeker, L.J. Segerlind, Trans. ASAE **19**, 346 (1976)
30. M. Akyurt, G.L. Zachariah, C.G. Haugh, Trans. ASAE **15**, 766 (1972)
31. R.E. Pitt, H.L. Chen, Trans. ASAE **26**, 1275 (1983)
32. N. Mohsenin, *Physical Properties of Plant and Animal Materials*, 2nd edn. (Gordon and Breach Science Publishers, New York, 1986)
33. R. Lu, V.M. Puri, J. Rheol. **35**, 1209 (1991)
34. M. van Zeebroeck, E. Dintwa, E. Tijskens, H. Ramon, Postharvest Biology and Technology (2004), accepted
35. H. Deresiewicz, ASME J. Appl. Mech. **21**, 327 (1954)
36. M. Abramowitz, A. Irene, *Handbook of mathematical functions: with formulas, graphs, and mathematical tables*, 8th edn. (Dover New York, New York, 1972)
37. Y.C. Fung, *A First Course in Continuum Mechanics*, 3rd edn. (Prentice-Hall Inc., Englewood Cliffs, New Jersey, 1994)
38. N.V. Brilliantov, F. Spahn, J.M. Hertzsch, Phys. Rev. E **53**, 5382 (1996)